Evidence of a Nodal Line in the Superconducting Gap Symmetry of Noncentrosymmetric $ThCoC_2$

A. Bhattacharyya,[1,2,3,*] D. T. Adroja,[2,3,†] K. Panda,[1] Surabhi Saha,[4] Tanmoy Das,[4,‡] A. J. S. Machado,[5] O. V. Cigarroa,[5,6] T. W. Grant,[5,6] Z. Fisk,[6] A. D. Hillier,[2] and P. Manfrinetti[7]

[1]*Department of Physics, Ramakrishna Mission Vivekananda Educational and Research Institute, Belur Math, Howrah 711202, West Bengal, India*
[2]*ISIS Facility, Rutherford Appleton Laboratory, Chilton, Didcot Oxon, OX11 0QX, United Kingdom*
[3]*Highly Correlated Matter Research Group, Physics Department, University of Johannesburg, PO Box 524, Auckland Park 2006, South Africa*
[4]*Department of Physics, Indian Institute of Science, Bangalore 560012, India*
[5]*Escola de Engenharia de Lorena, Universidade de São Paulo, P.O.Box 116, Lorena, São Paulo, 12602-810, Brazil*
[6]*Department of Physics and Astronomy, University of California-Irvine, Irvine, CA 92697, USA*
[7]*Department of Chemistry, University of Genova, 16146 Genova, Italy*

(Dated: April 4, 2019)

I. TIME REVERSAL SYMMETRY

The time evolution of the zero field (ZF)$-\mu$SR spectra of $ThCoC_2$ is shown in Fig.S1 for $T = 0.4$ K and 3.5 K. In this relaxation experiment, any muons stopped on the silver sample holder gave a time independent background. No signature of precession is visible (either at 0.4 K or 3.5 K), ruling out the presence of a sufficiently large internal magnetic field as seen in magnetically ordered compounds. The only possibility is that the muon$-$spin relaxation is due to static, randomly oriented local fields associated with the electronic and nuclear moments at the muon site. The ZF$-\mu$SR data are well described in terms of the damped Gaussian Kubo-Toyabe (KT) function, $G_{z2}(t) = A_1 G_{KT}(t) e^{-\lambda t} + A_{bg}$ where $G_{KT}(t) = \left[\frac{1}{3} + \frac{2}{3}(1-\sigma_{KT}^2 t^2) e^{\frac{-\sigma_{KT}^2 t^2}{2}}\right]$ is Gaussian Kubo-Toyabe function, λ is the electronic relaxation rate, A_1 is the initial asymmetry, A_{bg} is the background. The parameters σ_{KT}, A_1, and A_{bg} are found to be temperature independent. It is evident from the ZF$-\mu$SR spectra that there is no noticeable change in the relaxation rates at 3.5 K ($\geq T_c$) and 0.4 K ($\leq T_c$). This indicates that the time-reversal symmetry is preserved upon entering the superconducting state. σ_{KT} accounts for the Gaussian distribution of static fields from nuclear moments (the second moment of field distribution is $H_\mu^2 = \sigma^2/\gamma_\mu^2$, with muon gyromagnetic ratio $\gamma_\mu = 135.53$ MHz/T). The fits of μSR spectra in Fig.S1 by the decay function gave $\sigma_{KT} = 0.31(7)$ μs^{-1} and $\lambda = 0.12(6)$ μs^{-1} at 3.5 K and $\sigma_{KT} = 0.30(7)$ μs^{-1} and $\lambda = 0.11(9)$ μs^{-1} at 0.4 K. The fits are shown by the solid lines in Fig.S1. Since within the error bars both σ_{KT} and λ at $T < T_c$ and $T > T_c$ are similar, there is no evidence of time-reversal symmetry breaking in $ThCoC_2$. This result also confirm the absence of any kind of magnetic impurity in our sample. In Table I, we have given the fitted parameters obtained from the fit to the $\lambda^{-2}(T)$ data of $ThCoC_2$ using different gap models.

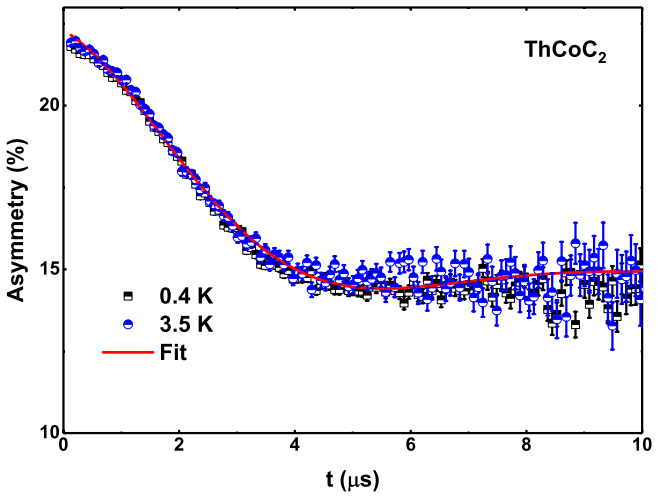

FIG. S1: (Color online) (a) Time dependence asymmetry spectra at 0.4 K and 3.5 K measured in zero magnetic field of $ThCoC_2$ with $T_c = 2.3$ K. The lines are the results of the fits. The absence of extra relaxation below T_c indicates no internal magnetic fields and, consequently, suggests that the superconducting state preserves time reversal symmetry.

TABLE I. Fitted parameters obtained from the fit to the $\lambda^{-2}(T)$ data of $ThCoC_2$ using different gap models.

Model	g(ϕ)	Gap Value $\Delta(0)$(meV)	Gap to T_c ratio $2\Delta(0)/k_B T_C$	χ^2
d-wave	cos(2ϕ)	0.77	7.80	3.45
$s+s$ wave	1	0.52; 0.07	5.22;0.74	5.01
s-wave	1	0.53	5.32	7.98

II. DFT CALCULATION

For the first-principles electronic structure calculation, we used the Vienna *ab initio* Simulation Package

(VASP) [1] and use the Perdew-Burke-Ernzerhof (PBE) form for the exchange-correlation functional [2]. The projector augmented wave (PAW) pseudo-potentials are used to describe the core electrons [3]. Electronic wave-functions are expanded using plane waves up to cut-off energy of 500 eV. The Monkhorst-Pack k-mesh is set to $14 \times 14 \times 14$ in the Brillouin zone for the self-consistent calculation. All atoms are relaxed in each optimization cycle until atomic forces on each atom are smaller than 0.001 eV nm. The lattice constants are obtained by relaxing the structure and with total energy minimization. Our obtained relaxed lattice parameters are $a = 0.38493$ nm, $b = 0.38493$ nm, $c = 0.39462$ nm, which are close to the experimental values [4, 5]. To deal with the strong correlation effect of the d-electrons of the Th and Co atoms, we employed LDA+U method with $U = 5$ eV on both atoms. We have recalculated the band structure with spin-orbit coupling, and no considerable change is obtained in the low-energy bands of present interests. We also did calculations for $U = 3$ eV and 7 eV to check the effect of U on the band structure (see Fig. 2S(c)).

II. DETAILS OF PAIRING EIGENVALUE CALCULATIONS

Our calculation of pairing interaction and pairing eigenvalue originating from spin-fluctuation is done by directly including the DFT band structure in a three-dimensional Brillouin zone (BZ). We start with a single-band Hubbard model, as dictated by the DFT calculation, which is given by

$$H = \sum_{\mathbf{k},\sigma=\uparrow,\downarrow} \xi_{\mathbf{k}} c^{\dagger}_{\mathbf{k}\sigma} c_{\mathbf{k}\sigma} + U \sum_{\mathbf{k},\mathbf{k}',\mathbf{q}} c^{\dagger}_{\mathbf{k}\uparrow} c_{\mathbf{k}+\mathbf{q}\uparrow} c^{\dagger}_{\mathbf{k}'\downarrow} c_{\mathbf{k}'-\mathbf{q}\downarrow}, \tag{1}$$

where $c^{\dagger}_{\mathbf{k}\sigma}(c_{\mathbf{k}\sigma})$ is the creation (annihilation) operator for non-interacting electron with momentum $\mathbf{k}$, and spin $\sigma = \uparrow / \downarrow$, and $\xi_{\mathbf{k}}$ is the corresponding band structure, taken directly from the DFT calculation. The second term is the Hubbard interaction, written in the band basis with the onsite potential U. Perturbative expansion of the Hubbard term in the spin-singlet and spin-triplet pairing channels yields,

$$H = \sum_{\mathbf{k},\sigma=\uparrow,\downarrow} \xi_{\mathbf{k}} c^{\dagger}_{\mathbf{k}\sigma} c_{\mathbf{k}\sigma} + \sum_{\mathbf{k}\mathbf{k}',\sigma\sigma'} V_{\sigma\sigma'}(\mathbf{k}-\mathbf{k}') c^{\dagger}_{\mathbf{k}\sigma} c^{\dagger}_{-\mathbf{k}\sigma'} c_{-\mathbf{k}'\sigma'} c_{\mathbf{k}'\sigma}. \tag{2}$$

Here $V_{\sigma\sigma'}$ refers to the spin singlet and triplet case when $\sigma = \mp\sigma$, respectively. The corresponding (static) pairing potentials are given in Eqs.(2-3) in the main text. The bare susceptibility is

$$\chi^0(\mathbf{q},\omega) = -\sum_{\mathbf{k}} \frac{f(\xi_{\mathbf{k}}) - f(\xi_{\mathbf{k}+\mathbf{q}})}{\omega - \xi_{\mathbf{k}} + \xi_{\mathbf{k}+\mathbf{q}} + \iota\delta}, \tag{3}$$

where f is the corresponding Fermi-function, and δ is an infinitesimal number. Since we are interested in the static limit of the pairing potential, the imaginary part of the above particle-hole correlator does not contribute and we obtain a real pairing potential V. In the RPA channel, the spin and charge channels are decoupled, and due to different denominators $1 \mp U\chi^0$, the spin channel is strongly enhanced while simultaneously charge channel is suppressed. The method is a weak to intermediate coupling approach and thus the value of U is restricted by the non-interacting bandwidth. We use $U = 400$ meV in our numerical calculation and the result is reproduced with different values of U. We note that this value of U is defined in the band basis, while the LDA+U is for the orbitals. The k-dependent of the pairing eigenfunction is dictated by the anisotropy in $V(\mathbf{q})$ which is directly related to the bare FS nesting character, this result remains unaffected by a particular choice of U in the weak to intermediate coupling range. With increasing U, the overall strength of V mainly increases and thus the pairing eigenvalue λ also increases. Since in this work, we are primarily interested in uncovering the pairing eigenfunction, the value of U remains irrelevant in this coupling strength.

From interacting Hamiltonian, we define the SC gap equation as [6–9],

$$\Delta_{\mathbf{k}} = -\sum_{\mathbf{k}'} V_{\sigma\sigma'}(\mathbf{k}-\mathbf{k}') \langle c_{-\mathbf{k}'\sigma} c_{\mathbf{k}'\sigma'} \rangle, \tag{4}$$

$$= -\sum_{\mathbf{k}'} V_{\sigma\sigma'}(\mathbf{k}-\mathbf{k}') \frac{\Delta_{\mathbf{k}'}}{2\xi_{\mathbf{k}'}} \tanh\left(\frac{\xi_{\mathbf{k}'}}{k_B T_c}\right) \tag{5}$$

In the limit $T \to 0$ we have $\langle c_{-\mathbf{k}\sigma} c_{\mathbf{k}\sigma'} \rangle \to \lambda \Delta_{\mathbf{k}}$, leading to an eigenvalue equation as

$$\Delta_{\mathbf{k}} = -\lambda \sum_{\mathbf{k}'} V_{\sigma\sigma'}(\mathbf{k}-\mathbf{k}') \Delta_{\mathbf{k}'}.$$

We solve this equation separately for spin singlet ($\sigma = -\sigma'$), and spin triplet ($\sigma = \sigma'$) cases. Since we restrict ourselves to the static limit, the above equation is solved for only Fermi momenta $\mathbf{k}_F$, $\mathbf{k}'_F$ in which $V_{\sigma\sigma'}(\mathbf{k}_F - \mathbf{k}'_F)$ becomes a $n \times n$ matrix with n being the number of discrete Fermi momenta considered in a 3D BZ.

We had presented results for $U = 5$ eV for both Th-d and Co-d orbital. Now we have carried out the U-dependence of the band structure as shown in Fig. S2 in the supplementary material. For a large variation of U from 3 eV to 7 eV, we find a systematic shift of the overall band structure. This changes the size of the Fermi surface but does not produce any topological change in it. The nesting wave vector, which dictates the pairing symmetry in our model, is aligned between the two flat areas of the Fermi surface along the $\mathbf{k}_z$ direction. Therefore, the systematic changes in the Fermi surface may only change the quantitative value of the nesting wave vector, but

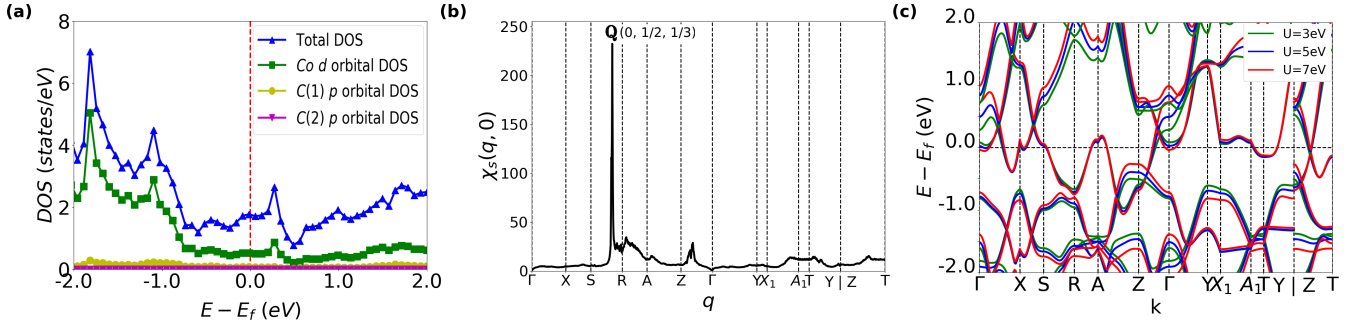

FIG. S2: (Color online) (a) Compute partial density of states (pDOS) plotted for three relevant orbitals near the Fermi level. We clearly observe that Co-d orbitals dominate the low-energy states. (b) The real part of the RPA susceptibility (static) in the spin-channel is plotted to the same high-symmetric directions. We observe a distinctly sharp peak at **Q** (0,1/2,1/3) in the susceptibility. This nesting peaks connect two Fermi surfaces across the $\mathbf{k_z} = 0$ plane. (c) Computed band structures for three different values of U. We notice a gradual shift of the bands, inducing a change in the FS area, but no change in the Fermi surface topology is observed in this wide range of U. $U = 5$ (middle plot) is used in the paper.

qualitatively it remains the same. Therefore, the pairing eigenfunction also remains the same. In summary, for the single band Fermi surface topology of this system, the nesting driven pairing symmetry is a robust result to the practical range of U used here.

* amitava.bhattacharyya@rkmvu.ac.in
† devashibhai.adroja@stfc.ac.uk
‡ tnmydas@gmail.com

[1] G. Kresse, and J. Furthmuller, Phys. Rev. B **54**, 11169 (1996).
[2] J. P. Perdew, K. Burke, and M. Ernzerhof, Phys. Rev. Lett. **77**, 3865 (1996).
[3] G. Kresse, and D. Joubert, Phys. Rev. B **59**, 1758 (1999).
[4] M. H. Gerss and W. Jeitschko, Mat. Res. Bull., **21**, 209-216 (1986).
[5] T. Grant, A. J. S. Machado, D. J. Kim, and Z. Fisk, Supercond. Sci. Technol. **27**, 035004 (2014).
[6] D. J. Scalapino, E. Loh, Jr., and J. E. Hirsch, Phys. Rev. B **34**, 8190 (R) (1986); T. M. Rice and K. Ueda, Phys. Rev. B 34, 6420 (1986); J. R. Schrieffer, X. G. Wen, and S. C. Zhang, Phys. Rev. B **39**, 11663 (1989); P. Monthoux, A. V. Balatsky, and D. Pines, Phys. Rev. Lett. **67**, 3448 (1991); Manfred Sigrist and Kazuo Ueda, Rev. Mod. Phys. **63**, 239 (1991); D. J. Scalapino, Rev. Mod. Phys. **84**, 1383 (2012).
[7] P. J. Hirschfeld, M. M. Korshunov, and I. I. Mazin, Rep. Prog. Phys. **74**, 124508 (2011); S. Graser, T. A. Maier, P. J. Hirschfeld and D. J. Scalapino, New J. Phys. **11**, 025016 (2009); T. Das and A. V. Balatsky, Phys. Rev. B **84**, 014521 (2011); Zi-Jian Yao, Jian-Xin Li, and Z. D. Wang, New J. Phys., **11**, 025009 (2009).
[8] T. Das, J.-X. Zhu and M. J. Graf, Sci. Rep. **5,** 8632 (2015); H. Ikeda, M.-T. Suzuki and R. Arita, Phys. Rev. Lett. **114**, 147003 (2015).
[9] Katsunori Kubo, Phys. Rev. B **75**, 224509 (2007).